Since January 2020 Elsevier has created a COVID-19 resource centre with free information in English and Mandarin on the novel coronavirus COVID-19. The COVID-19 resource centre is hosted on Elsevier Connect, the company's public news and information website.

available at www.sciencedirect.com

SCIENCE DIRECT®

journal homepage: http://www.elsevier.com/locate/ecocom

On representing network heterogeneities in the incidence rate of simple epidemic models

Manojit Roy *, *Mercedes Pascual*

Department of Ecology and Evolutionary Biology, 830 North University Avenue, University of Michigan, Ann Arbor, MI 48109, United States

ARTICLE INFO

Article history:
Received 30 June 2005
Received in revised form
9 September 2005
Accepted 10 September 2005
Published on line 19 January 2006

Keywords:
Epidemics
SIRS
Network
Small-world
Fluctuations
Cycles

ABSTRACT

Mean-field ecological models ignore space and other forms of contact structure. At the opposite extreme, high-dimensional models that are both individual-based and stochastic incorporate the distributed nature of ecological interactions. In between, moment approximations have been proposed that represent the effect of correlations on the dynamics of mean quantities. As an alternative closer to the typical temporal models used in ecology, we present here results on ''modified mean-field equations'' for infectious disease dynamics, in which only mean quantities are followed and the effect of heterogeneous mixing is incorporated implicitly. We specifically investigate the previously proposed empirical parameterization of heterogeneous mixing in which the bilinear incidence rate SI is replaced by a nonlinear term kS^pI^q, for the case of stochastic SIRS dynamics on different contact networks, from a regular lattice to a random structure via small-world configurations. We show that, for two distinct dynamical cases involving a stable equilibrium and a noisy endemic steady state, the modified mean-field model approximates successfully the steady state dynamics as well as the respective short and long transients of decaying cycles. This result demonstrates that early on in the transients an approximate power-law relationship is established between global (mean) quantities and the covariance structure in the network. The approach fails in the more complex case of persistent cycles observed within the narrow range of small-world configurations.

1. Introduction

Most population models of disease (Anderson and May, 1992) assume complete homogeneous mixing, in which an individual can interact with all others in the population. In these well-mixed models, the disease incidence rate is typically represented by the term βSI that is bilinear in S and I, the number of susceptible and infective individuals (Bailey, 1975), β being the transmission coefficient. With these models it has been possible to establish many important epidemiological results, including the existence of a population threshold for the spread of disease and the vaccination levels required for eradication (Kermack and McKendrick, 1927; Anderson and May, 1992; Smith et al., 2005). However, individuals are discrete and not well-mixed; they usually interact with only a small subset of the population at any given time, thereby imposing a distinctive contact structure that cannot be represented in mean-field models. Explicit interactions within discrete spatial and social neighborhoods have been incorporated into a variety of individual-based models on a spatial grid and on networks (Bolker and Grenfell, 1995; Johansen, 1996; Rhodes and Anderson, 1996; Keeling, 1999; Pastor-Satorras and Vespignani, 2001; Newman, 2002; Sander et al., 2002; Van Baalen, 2002; Koopman, 2004; Shirley and Rushton,

* Corresponding author. Present address: Department of Zoology, 223 Bartram Hall, PO Box 118525, University of Florida, Gainesville, FL 32611, United States. Tel.: +1 352 392 1040; fax: +1 352 392 3704.
E-mail addresses: roym@ufl.edu (M. Roy), pascual@umich.edu (M. Pascual).
1476-945X/$ – see front matter
doi:10.1016/j.ecocom.2005.09.001

2005). Simplifications of these high-dimensional models have been developed to better understand their dynamics, make them more amenable to mathematical analysis and reduce computational complexity (Keeling, 1999; Eames and Keeling, 2002; Franc, 2004). These approximations are based on moment closure methods and add corrections to the mean-field model due to the influence of covariances, as well as equations for the dynamics of these second order moments (Pacala and Levin, 1997; Bolker, 1999; Brown and Bolker, 2004).

We address here an alternative simplification approach closer to the original mean-field formulation, which retains the basic structure of the mean-field equations but incorporates the effects of heterogeneous mixing implicitly via modified functional forms (McCallum et al., 2001). Specifically, the bilinear transmission term (SI) in the well-mixed equations is replaced by a nonlinear term S^pI^q (Severo, 1969), where the exponents p, q are known as ''heterogeneity parameters''. This formulation allows an implicit representation of distributed interactions when the details of individual-level processes are unavailable (as is often the case, see Gibson, 1997), and when field data are collected in the form of a time series (e.g., Koelle and Pascual, 2004). We henceforth refer to these modified equations as the *heterogeneous mixing*, or ''HM'', model following Maule and Filipe (in preparation). The HM model is known to exhibit important properties not observed in standard mean-field models, such as the presence of multiple equilibria and periodic solutions (Liu et al., 1986, 1987; Hethcote and van den Driessche, 1991; Hochberg, 1991). This model has also been successfully fitted to the experimental time series data of lettuce fungal disease to explain its persistence (Gubbins and Gilligan, 1997). However, it is not well known whether these modified mean-field equations can indeed approximate the population dynamics that emerge from individual level interactions. Motivated by infectious diseases of plants, Maule and Filipe (in preparation) have recently compared the dynamics of the HM model to a stochastic susceptible-infective (SI) model on a spatial lattice.

In this paper, we implement a stochastic version of the susceptible-infective-recovered-susceptible (SIRS) dynamics, to consider a broader range of dynamical behaviors including endemic equilibria and cycles (Bailey, 1975; Murray, 1993; Johansen, 1996). Recovery from disease leading to the development of temporary immunity is also relevant to many infectious diseases in humans, such as cholera (Koelle and Pascual, 2004). For the contact structure of individuals in the population we use a small-world algorithm, which is capable of generating an array of configurations ranging from a regular grid to a random network (Watts and Strogatz, 1998). Theory on the structural properties of these networks is well developed (Watts, 2003), and these properties are known to exist in many real interaction networks (Dorogotsev and Mendes, 2003). A small-world framework has also been used recently to model epidemic transmission processes of severe acute respiratory syndrome or SARS (Masuda et al., 2004; Verdasca et al., 2005).

We demonstrate that the HM model can accurately approximate the endemic steady states of the stochastic SIRS system, including its short and long transients of damped cycles under two different parameter regimes, for all configurations between the regular and random networks. We show that this result implies the establishment early on in the transients of a double power-law scaling relationship between the covariance structure on the network and global (mean) quantities at the population level (the total numbers of susceptible and infective individuals). We also demonstrate the existence of a complex dynamical behavior in the stochastic system within the narrow small-world region, consisting of persistent cycles with enhanced amplitude and a well-defined period that are not predicted by the equivalent homogeneous mean-field model. In this case, the HM model captures the mean infection level and the overall pattern of the decaying transient cycles, but not their phases. The model also fails to reproduce the persistence of the cycles. We conclude by discussing the potential significance and limitations of these observations.

2. The model

2.1. Stochastic formulation

2.1.1. The network

The population structure, that is, the social contact pattern among individuals in the population, is modeled using a small-world framework as follows. We start with a spatial grid with the interaction neighborhood restricted to eight neighbors (Fig. 1A) and periodic boundary condition, and randomly rewire a fraction ϕ of the local connections (avoiding self and multiple connections) such that the average number of connections per individual is preserved at n_0 (=8 in this case). We call ϕ the ''short-cut'' parameter of the network. This is a two-dimensional extension of the algorithm described in Watts and Strogatz (1998). As pointed out by Newman and Watts (1999), a problem with these algorithms is the small but finite probability of the existence of isolated sub-networks. We consider only those configurations that are completely connected. For $\phi = 0$ we have a regular grid (Fig. 1A), whereas $\phi = 1$ gives a random network (Fig. 1C). In between these extremes, there is a range of ϕ values near 0.01 within which the network exhibits *small-world* properties (Fig. 1B). In this region, most local connections remain intact making the network highly ''clustered'' like the regular grid, with occasional short-cuts that lower the average distance between nodes drastically as in the random network. These properties are illustrated with two quantities, the ''clustering coefficient'' C and the ''average path length'' L (Watts, 2003). C denotes the probability that two neighbors of a node are themselves neighbor, and L denotes the average shortest distance between two nodes in the network. The small-world network exhibits the characteristic property of having a high value of C and simultaneously a low value of L (Fig. 1D).

2.1.2. SIRS dynamics

Once the network structure is generated using the algorithm described above, the stochastic SIRS dynamics are implemented with the following rules:

- A susceptible individual gets infected at a rate $n_I\beta$, where n_I is the number of infective neighbors and β is the rate of

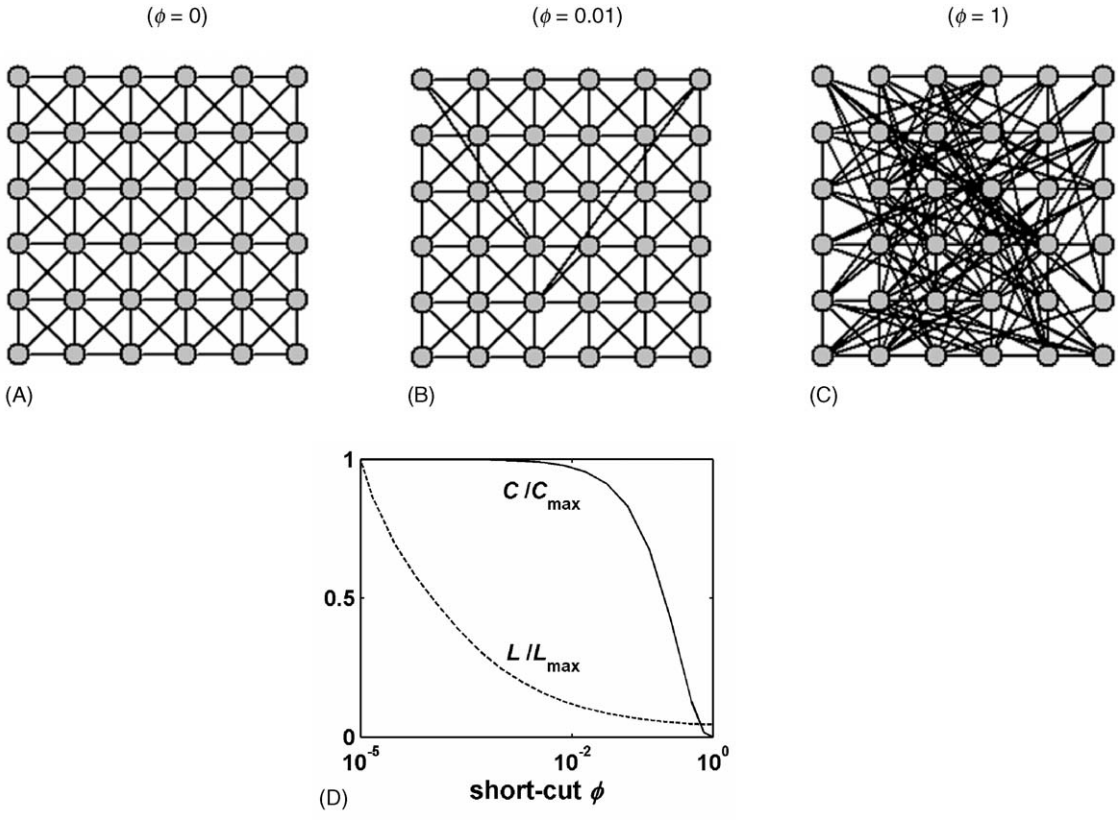

Fig. 1 – Diagrams of three network configurations with $\phi = 0$ (regular grid), $\phi = 0.01$ (small-world network) and $\phi = 1$ (random network) are illustrated respectively in A–C. Panel D shows the clustering coefficient C and the average path length L (normalized by their respective maxima C_{max} and L_{max}) against the short-cut parameter ϕ (horizontal axis is on log scale). In the small-world regime (near $\phi = 0.01$) the network displays the characteristic properties of high C and low L.

disease transmission across a connected susceptible-infective pair.
- An infective individual loses infection at a rate γ and recovers temporarily.
- A recovered individual loses its temporary immunity at a rate δ and becomes susceptible again.

Stochasticity arises because the rate of each event specifies a stochastic process with a Poisson-distributed time-intervals between successive occurrences of the event, with a mean interval of $(\text{rate})^{-1}$. Total population size is assumed constant (demography and disease-induced mortality are not considered), and infection propagates from an infective to a susceptible individual only if the two are connected. Correlations develop as the result of the local transmission rules and the underlying network structure. Therefore, holding β, γ and δ constant while varying the short-cut parameter ϕ allows us to explore the effects of different network configurations (such as Fig. 1A–C) on the epidemic.

2.2. *Analytical considerations*

2.2.1. *Pair-wise formulation*

One way to analytically treat the above stochastic system is by using a pair-wise formulation (Keeling, 1999), which considers partnerships as the fundamental variables, and incorporates the pair-wise connections into model equations. Using the notations of Keeling et al. (1997), this formulation gives the following set of equations for the dynamics of disease growth,

$$\frac{d[S^n]}{dt} = -\beta \sum_m [S^n I^m] + \delta[R^n], \qquad \frac{d[I^n]}{dt} = \beta \sum_m [S^n I^m] - \gamma[I^n],$$
$$\frac{d[R^n]}{dt} = \gamma[I^n] - \delta[R^n]$$

where $[S^n]$, $[I^n]$ and $[R^n]$ denote respectively the number of susceptible, infective and recovered individuals each with exactly n connections, and $[S^n I^m]$ denotes the number of connected susceptible-infective pairs with n and m connections. By writing $\sum_n [S^n] = [S] = S$, where S is the total number of susceptible individuals, and $\sum_n \left(\sum_m [S^n I^m]\right) = \sum_n [S^n I] = [SI]$, where $[SI]$ denotes the total number of connected susceptible-infective pairs, we can rewrite the equations for the number of susceptible, infective and recovered individuals as

$$\frac{dS}{dt} = -\beta[SI] + \delta R, \qquad \frac{dI}{dt} = \beta[SI] - \gamma I, \qquad \frac{dR}{dt} = \gamma I - \delta R \tag{1}$$

Even though this set of equations is exact, it is not closed and additional equations are needed to specify the dynamics of the $[SI]$ pairs, which in turn depend on the dynamics of triples, etc., in an infinite hierarchy that is usually closed by

moment closure approximations. However, a satisfactory closure scheme for a locally clustered network is still lacking (but see Keeling et al., 1997; Rand, 1999).

2.2.2. *The heterogeneous mixing (HM) model*

Here we pursue a different avenue to approximate the stochastic system with modified mean-field equations, which consider only the dynamics of mean quantities but replace the standard bilinear term βSI with a nonlinear transmission rate as follows,

$$\frac{dS}{dt} = -\beta k S^p I^q + \delta R, \qquad \frac{dI}{dt} = \beta k S^p I^q - \gamma I, \qquad \frac{dR}{dt} = \gamma I - \delta R \tag{2}$$

where k, p, q are the "heterogeneity" parameters (Severo, 1969; Liu et al., 1986; Hethcote and van den Driessche, 1991; Hochberg, 1991). We call Eq. (2) the "heterogeneous mixing" (HM) model (Maule and Filipe, in preparation).

We note from Eq. (1) that the incidence rate of the epidemic can be estimated by counting the number of connected susceptible-infective pairs $[SI]$ in the network. Furthermore, $[SI]$ is directly related to the correlation C_{SI} that arises between susceptible and infective individuals in the network (Keeling, 1999). Therefore, comparing Eqs. (2) with (1) we see that the HM model implicitly assumes a double power-law relationship between this covariance structure and the abundances of infective and susceptible individuals. For instance, in a homogeneous network (such as a regular grid) with identical number of connections n_0 for all individuals, we have

$$C_{SI} = \frac{N}{n_0}\frac{[SI]}{SI} \propto k S^{p-1} I^{q-1}, \tag{3}$$

where $N = S + I + R$ is the population size (Keeling, 1999). Relationships such as Eq. (3) provide an important first step towards understanding how the phenomenological parameters k, p and q are related to network structure.

2.2.3. *A mean-field approximation*

For a homogeneous random network in which every individual is connected to exactly n_0 randomly distributed others (see Appendix A), the susceptible and infective individuals are uncorrelated and the total number of interacting pairs $[SI] = (n_0/N)SI$. Eq. (1) then reduce to

$$\frac{dS}{dt} = -\beta\frac{n_0}{N} SI + \delta R, \qquad \frac{dI}{dt} = \beta\frac{n_0}{N} SI - \gamma I, \qquad \frac{dR}{dt} = \gamma I - \delta R \tag{4}$$

These equations incorporate the familiar bilinear term SI for the incidence rate, and provide a mean-field approximation for the stochastic system in which each individual randomly mixes with n_0 others. Note that the transmission coefficient β is proportionately reduced by a factor n_0/N, which is the fraction of the population in a contact neighborhood of each individual. In a completely well-mixed population, $n_0 = N$, and these equations reduce to the standard Kermack–McKendrick form (Kermack and McKendrick, 1927). Eq. (4) exhibit either a disease-free equilibrium, $I(t) = 0$, or an endemic equilibrium, $I(t) = [\delta N/(\gamma + \delta)][1 - \gamma/\beta n_0]$, depending on whether the basic reproductive ratio $R_0 = n_0\beta/\gamma$ is less or greater than unity. It is to be noted that while Eq. (4) describe a homogeneous random network exactly, it provides only an approximation for the random network with $\phi = 1$, in which individuals have a binomially distributed number of connections around a mean n_0 (Appendix A).

3. Method

Details of the implementation of the stochastic system are described in Appendix B. One practical approach to estimate the parameters k, p and q of the HM model, when the individual-level processes are unknown, would be to fit these parameters using time series data (Gubbins and Gilligan, 1997; Bjørnstad et al., 2002; Finkenstädt et al., 2002). Indeed, with a sufficient number of parameters a satisfactory agreement between the model and the data is almost always possible. A direct fit of time series, however, will not tell us whether the disease transmission rate is well approximated by the functional form kS^pI^q of the model. We instead fit the parameters k, p, q to the transmission rate "observed" in the output of the stochastic simulation. Specifically, we obtain least-squared estimates of k, p, q by fitting the term kS^pI^q to the computed number of pairs $[SI]$ that gives the disease transmission rate of the stochastic system (see Eq. (1)). We then incorporate these estimates in Eq. (2), and compare the infective time series produced by this HM model to that generated by the original stochastic network simulation. Fig. 2 illustrates the method using the regular grid as an

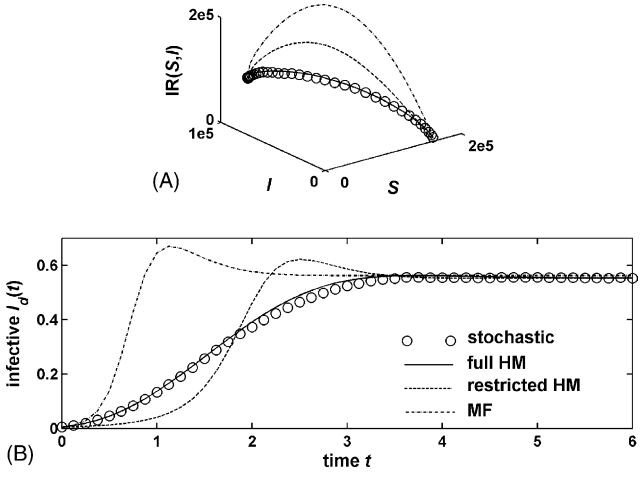

Fig. 2 – The method discussed in Section 3 is illustrated for a regular grid ($\phi = 0$). (A) The incidence rate (IR) of the stochastic system is obtained for a single run of the dynamics from time $t = 0$ up to $t = 20{,}000$, by plotting the number of $[SI]$ pairs against the numbers S and I of susceptible and infective individuals computed from the each snapshot of the network. Values of the epidemic parameters are $\beta = \gamma = 1$, $\delta = 1.8$. Least-squared fits of the functional forms kS^pI^q and $(n_0/N)S^{p_r}I^{q_r}$ of the full and restricted HM models, and $(n_0/N)SI$ of the bilinear mean-field (MF) approximation are overlaid. (B) Simulated infective time series ($I_d(t) \equiv I(t)/N$) for the stochastic system is plotted together with the solutions of the three population models, to examine the accuracy of these approximations.

example. In this way, we can address whether the transmission rate is well captured by the modified functional form, and if that is the case, whether the HM model approximates successfully the aggregated dynamics of the stochastic system.

We compare the stochastic simulation with the predictions of three sets of model equations, representing different degrees of approximation of the system. Besides the HM model described above, we consider the bilinear mean-field model given by Eq. (4), which assumes $k = n_0/N$ and $p = q = 1$. This comparison demonstrates the inadequacy of the well-mixed assumption built into the bilinear formulation. We also discuss a restricted HM model with an incidence function of the form $(n_0/N)S^{p_r}I^{q_r}$ in Eq. (2), with only two heterogeneity parameters p_r and q_r, as originally proposed by Severo (1969) and studied by Liu et al. (1986), Hethcote and van den Driessche (1991) and Hochberg (1991).

4. Results

The stochastic SIRS dynamics are capable of exhibiting a diverse array of dynamical behaviors, determined by both the epidemic parameters β, γ, δ and the network short-cut parameter ϕ. We choose the following three scenarios:

- *Stable equilibrium*: Infection levels in the population reach a stable equilibrium relatively rapidly after a short transient (Fig. 3A).
- *Noisy endemic state*: Infection levels exhibit stochastic fluctuations around an endemic state following a long transient of decaying cycles (Fig. 3B).
- *Persistent cycles*: Fluctuations with a well defined period and enhanced amplitude persist in the small-world region near $\phi = 0.01$ (Fig. 3B).

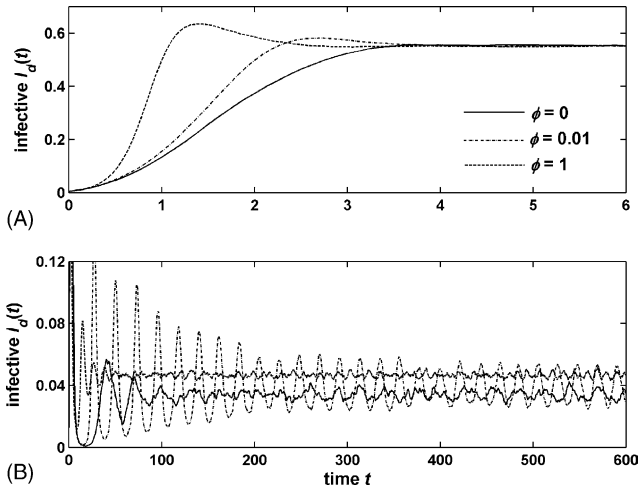

Fig. 3 – Examples of infective time series $I_d(t)$ for the stochastic system in two dynamical regimes are shown for three values of ϕ. (A) Stable equilibrium following a short transient is plotted for $\beta = \gamma = 1$, $\delta = 1.8$. (B) Decaying oscillations onto a noisy endemic state for $\beta = \gamma = 1$, $\delta = 0.065$. Persistent cycles with enhanced amplitude occur in the small-world network ($\phi = 0.01$).

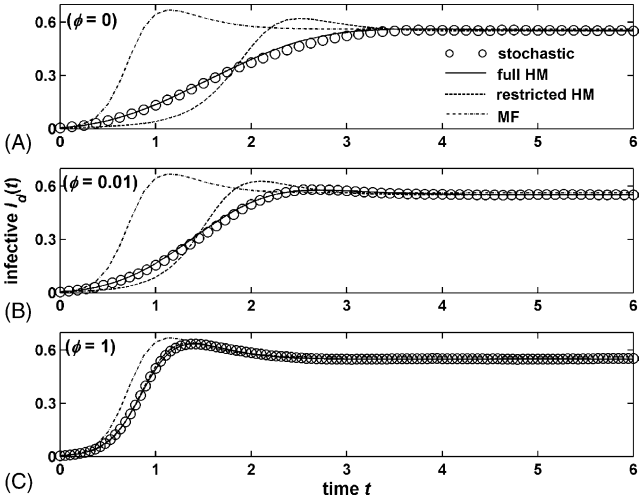

Fig. 4 – Time series generated by the two HM models and the mean-field equations are compared with the stochastic simulation data for the dynamics with a stable equilibrium (A is same as Fig. 2B). For the random network ($\phi = 1$) the predictions of the two HM models coincide with the simulation.

The reason for choosing these different temporal patterns is to test the HM model against a wider range of behaviors of the stochastic system. The oscillatory case has epidemiological significance because of the observed pervasiveness of cyclic disease patterns (Cliff and Haggett, 1984; Grenfell and Harwood, 1997; Pascual et al., 2000).

4.1. *Stable equilibrium*

Fig. 3A presents simulation examples of the epidemic time series for three values of the short-cut parameter ϕ, representing the regular grid ($\phi = 0$), the small-world network ($\phi = 0.01$) and the random network ($\phi = 1$). The transient pattern depends strongly on ϕ: a high degree of local clustering in a regular grid slows the initial buildup of the epidemic, whereas in a random network with negligible clustering (Fig. 1D) the disease grows relatively fast. The transient for the small-world network lies in between these two extremes. By contrast, the stable equilibrium level of the infection remains insensitive to ϕ, implying that the equilibrium should be well predicted by the bilinear mean-field approximation (Eq. (4)) itself.

Least-squared estimates of the two sets of heterogeneity parameters $[k, p, q]$ and $[k_r = n_0/N, p_r, q_r]$, for the full and restricted versions of the HM model respectively, are obtained for a series of ϕ values corresponding to different network configurations, as described in Section 3. The disease parameters β, γ and δ are kept fixed throughout, making the epidemic processes operate at the same rates across different networks, so that the effects of the network structure on the dynamics can be studied independently. Fig. 4 illustrates the comparison of model predictions with stochastic simulations shown in Fig. 3A. The time series generated by the mean-field Eq. (4) is also overlaid. Clearly the mean-field model suffices to predict the equilibrium of all three examples, as noted earlier. Approximation of the

transient patterns, however, presents a different picture. The mean-field trajectory deviates the most from the stochastic simulation for the regular grid ($\phi = 0$), and the least for the random network ($\phi = 1$). The full HM model with its three parameters k, p and q, on the other hand, demonstrates an excellent agreement with the stochastic transients for all values of ϕ. By comparison, the transient patterns of the restricted HM model with only two fitting parameters p_r and q_r differ significantly for low values of ϕ (Fig. 4A and B). The poor agreement of the restricted HM and the mean-field transients with the stochastic data for a clustered network (low ϕ) is due to the failure of their respective incidence functions to fit the transmission rate of the stochastic system (Fig. 2A).

On the other hand, the random network has negligible clustering, and the interaction between susceptible and infective individuals is sufficiently well mixed for the restricted HM model to provide as good an approximation of the stochastic transient as the full HM model (Fig. 4C). The estimates $[k,\ p,\ q] = [0.0001,\ 0.94,\ 0.97]$ and $[n_0/N,\ p_r,\ q_r] = [0.00005,\ 0.99,\ 1]$ for these two models are also quite similar. The discrepancy for the mean-field transients (Fig. 4C) is due to the fact that the mean-field model gives only an approximate description of the random network with $\phi = 1$ as noted before. At the other extreme, for a regular grid the estimates of the full and restricted HM models are $[k,\ p,\ q] = [1.66, 0.3, 0.69]$ and $[n_0/N, p_r, q_r] = [0.00005, 0.84, 1.13]$, which differ considerably from each other.

Fig. 5A and B demonstrate how the parameters k, p and q of the full HM model depend on the short-cut parameter ϕ. All three of them approach their respective well-mixed values ($k = 0.00005$, $p = q = 1$) as $\phi \to 1$, and they deviate the most as $\phi \to 0$, in accord with the earlier discussion. In particular, k is significantly higher, and likewise p and q are lower, for the regular grid than a well-mixed system, implying a strong nonlinearity of the transmission mechanism in a clustered network. Such a large value of k can be understood within the context of the incidence function kS^pI^q, and explains why only two parameters, p_r and q_r in the restricted HM model, cannot absorb the contribution of k. In a homogeneous random network with n_0 connections per individual, the term $(n_0/N)SI$ gives the expected total number of pairs $[SI]$ that govern disease transmission in the network, and the exponent values $p = q = 1$ indicate random mixing (of susceptible and infective individuals). By contrast, local interactions in a clustered network lower the availability of susceptible individuals (infected neighbors of an infective individual act as a barrier to disease spread), resulting in a depressed value of the exponent p significantly below 1. This nonlinear effect, combined with a low initial infective number I_0 (0.5% of the total population randomly infected) requires k in the HM model to be large enough to match the disease transmission in the network. Indeed, as Table 1 demonstrates, both k and p are quite sensitive to I_0 for a regular grid, unlike the other exponent q that does not

Table 1 – Estimates of the parameters k, p and q for the full HM model and different initial proportions of infective individuals in the population, for the case of stochastic dynamics on a regular grid exhibiting stable equilibria (see text for details)

I_0/N	k	p	q
0.005	1.66	0.30	0.69
0.01	0.78	0.39	0.68
0.05	0.06	0.65	0.68
0.1	0.02	0.76	0.68

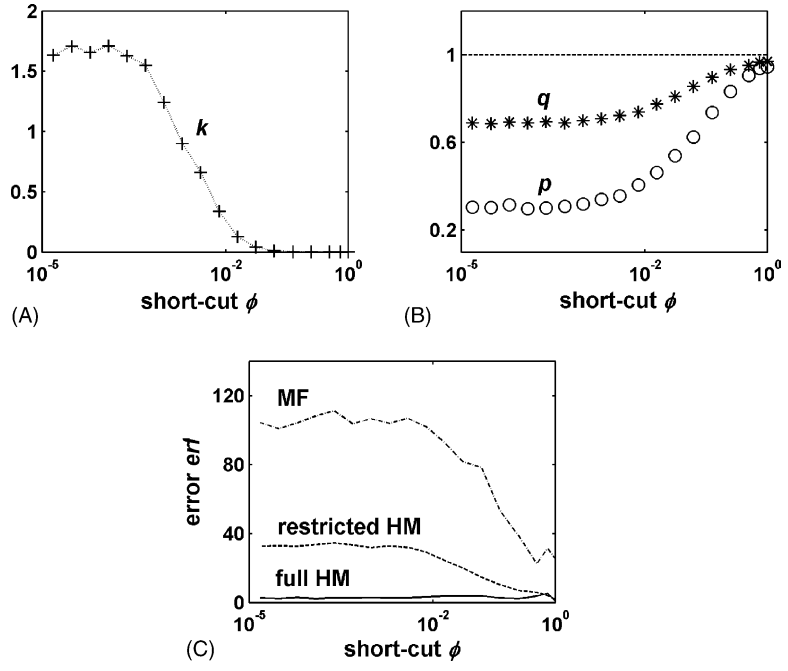

Fig. 5 – Panels A and B show estimates of the parameters k, p and q for the full HM model against ϕ (on a semilog axis) for the stable equilibrium dynamics. The dashed line in B shows the expected mean-field values. In C, the error function erf (Eq. (5)) is plotted against ϕ for the three epidemic models.

depend on initial conditions. Increasing I_0 facilitates disease growth by distributing infective and susceptible individuals more evenly, which causes an increase of the value of p and a compensatory reduction of k.

An interesting pattern in Fig. 5A and B is that the values of the heterogeneity parameters remain fairly constant initially for low ϕ, in particular within the interval $0 \leq \phi < 0.01$ for the exponents p and q (the range is somewhat shorter for k), and then start approaching respective mean-field values as ϕ increases to 1. This pattern of variation is reminiscent of the plot for the clustering coefficient C shown in Fig. 1D, and suggests that the clustering of the network, rather than its average path length L, influences disease transmission strongly.

A measure of the accuracy of the approximation can be defined by an error function erf, computed as a mean of the point-by-point deviation of the infective time series $I_m(t)$ predicted from the models, relative to the stochastic simulation data $I_s(t)$, over the length T of the transient (the equilibrium values of the models coincide with the simulation, see Fig. 4),

$$\text{erf} = \left(\frac{1}{T} \sum_{t=1}^{T} \frac{|I_m(t) - I_s(t)|}{I_s(t)} \right) \times 100, \tag{5}$$

(multiplication by 100 expresses erf as a percentage of the simulation time series). Fig. 5C shows erf as a function of ϕ for the three models. The total failure of the mean-field approximation to predict the stochastic transients is evident in the large magnitudes of error (it is 25% even for the random networks). By contrast, the excellent agreement of the full HM model for all ϕ results in a low error throughout. On the other hand, the restricted version of the HM model gives over 30% error for low ϕ whereas it is negligible for high ϕ. Interestingly, erf for the restricted HM and mean-field models show similar patterns of variation with ϕ as in Fig. 5B, staying relatively constant within $0 \leq \phi < 0.01$ and then decreasing relatively fast. Local clustering in a network with low ϕ causes disease transmission to deviate from a well-mixed approximation, and thus influences the pattern of erf for these simpler models.

4.2. *Stochastic fluctuations and persistent cycles*

The second type of dynamical behavior of the stochastic system exhibits a relatively long oscillatory transient that settles onto a noisy endemic state for most values of ϕ, near 0 as well as above (Fig. 3B). Stochastic fluctuations are stronger for $\phi = 0$ than $\phi = 1$. However, in a significant exception the cycles tend to persist with a considerably increased amplitude and well defined period for a narrow range of ϕ near 0.01, precisely where the small-world behavior arises in the network. Such persistent cycles are not predicted by the homogeneous epidemic dynamics given by Eq. (4), and are therefore a consequence of the correlations generated by the contact structure. To our knowledge such nonmonotonic pattern for the amplitude of the cycles with the network parameter ϕ has not been observed before (see Section 5 for a comparison of these results with those of other studies).

We estimate two quantities, the "coefficient of variation" (CV) and the "degree of coherence" (DC), which determine respectively the strength and periodicity of the cycles for different values of ϕ. CV has the usual definition

$$\text{CV} = \frac{\sqrt{(1/(T_S - 1)) \sum_{t=1}^{T_S} (I(t) - \bar{I})^2}}{\bar{I}}, \tag{6}$$

where the numerator denotes the standard deviation of the infective time series of length T_S (in the stationary state excluding transients), and the denominator denotes its mean over the same time length T_S. Fig. 6A exhibits a characteristic peak for CV near $\phi = 0.01$, demonstrating a maximization of the cycle amplitudes in the small-world region compared to both the high and low values of ϕ. The plot also shows that the fluctuations at the left side tail of the peak are stronger than its right side tail. Consistent with this pattern, sustained fluctuations in a stochastic SIRS model on a spatial grid ($\phi = 0$) were also shown by Johansen (1996). By contrast, the low variability in the random network ($\phi \to 1$) is due to the fact that the corresponding mean-field model (Eq. (4)) does not have oscillatory solutions.

DC provides a measure of the sharpness of the dominant peak in the Fourier power spectrum of the infective time series, and is defined as

$$\text{DC} = \frac{h_{\max}}{(\Delta\omega/\omega_{\max})}, \tag{7}$$

where $h_{\max}$, $\omega_{\max}$ and $\Delta\omega$ are the peak height, peak frequency and the width at one-tenth maximum respectively of a Gaussian fit to the dominant peak. The sharp nature of the peak, particularly for the small-world network, makes it unfeasible to use the standard "width at half-maximum"

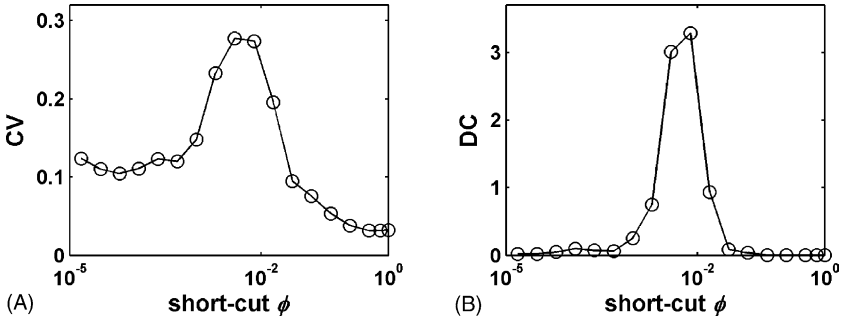

Fig. 6 – The coefficient of variation, CV (Eq. (6)), and the degree of coherence, DC (Eq. (7)), are plotted against ϕ in A and B, respectively (see text for definitions). Each point in B represents estimates using a Fourier power spectrum averaged over 10 independent realizations of the stochastic simulations.

(Gang et al., 1993; Lago-Fernández et al., 2000) which is often zero here. The modified implementation in Eq. (7) therefore considerably underestimates the sharpness of the dominant peak. Even then, Fig. 6B depicts a fairly narrow maximum for DC near $\phi = 0.01$, indicating that the cycles within the small-world region have a well-defined period. The low value of DC for $\phi = 0$ implies that the fluctuations in the regular grid are stochastic in nature.

A likely scenario for the origin of these persistent cycles is as follows. Stochastic fluctuations are locally maintained in a regular grid by the propagating fronts of spatially distributed infective individuals, but they are out of phase across the network. The infective individuals are spatially correlated over a length $\xi \propto \delta^{-1}$ in the grid (Johansen, 1996), which typically has a far shorter magnitude than the linear extent of the grid used here (increasing δ reduces the correlation length ξ further, which weakens these fluctuations and gives the stable endemic state observed for instance in Fig. 3A). The addition of a small number of short-cuts in a small-world network (Fig. 1B) couples together a few of these local fronts, thereby effectively increasing the correlation length to the order of the system size and creating a globally coherent periodic response. As more short-cuts are added, the network soon acquires a sufficiently random configuration and the homogeneous dynamics become dominant.

Another important point to note in Fig. 3B is that, in contrast to Fig. 3A, the mean infection level $\bar{I}$ of the cycles is not independent of ϕ: $\bar{I}$ now increases slowly with ϕ. An immediate implication of this observation is that, unlike the earlier case of a stable equilibrium, the bilinear mean-field model of Eq. (4) will no longer be able to accurately predict the mean infection for all ϕ. Fig. 7 shows the same examples of the stochastic time series as in Fig. 3B, along with the solutions of the three models. As expected, the mean-field time series fails to predict the mean infection level at varying degrees in all three cases, deviating most for the regular grid ($\phi = 0$) and least for the random network ($\phi = 1$). By comparison, the equilibrium solutions of the full and restricted versions of the HM model both demonstrate good agreement with the mean infection level of the stochastic system. For the transient patterns, the two HM models exhibit similar decaying cycles of roughly the same period, and also of the same transient length, as the stochastic time series but they occur at a different phase. Even though the transient cycles of the HM models persist the longest for $\phi = 0.01$, they eventually decay onto a stable equilibrium and thus fail to predict the persistent oscillations of the small-world network. The mean-field model, on the other hand, shows damped cycles of much shorter duration and hence is a poor predictor overall.

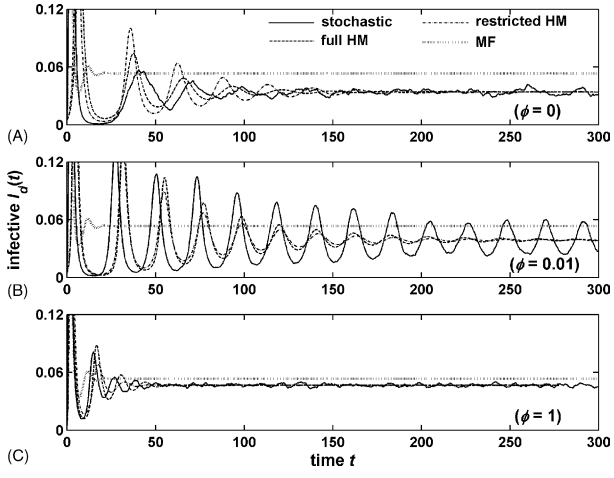

Fig. 7 – Model time series for the decaying cycles with $\beta = \gamma = 1$, $\delta = 0.065$ are compared with the stochastic simulation. The two HM models show good agreement for the mean infection level in the data. None reproduce the persistent cycles of the small-world network (in B).

The close agreement of the two HM time series with each other for $\phi = 0.01$ (Fig. 7B) is due to the fact that the least-squared estimate of k for the full HM model is 0.00005, equal to n_0/N of the restricted HM, and the exponents p, q likewise reduce to p_r, q_r. Within the entire range $0 \leq \phi \leq 1$, the estimates of p and p_r for the full and restricted HM models lie between [0.68, 1.08] and [0.82, 0.93], respectively, whereas q and q_r both stay close to a value of 1.1.

It is interesting to note here that a necessary condition for limit cycles in an SIRS dynamics with a nonlinear incidence rate S^pI^q is $q > 1$ (Liu et al., 1986), which both the full and restricted HM models appear to satisfy. One possible reason then for their failure to reproduce the cycles in the small-world region is the overall complexity of the stochastic time series, which results from nontrivial correlation patterns present in the susceptible-infective dynamics. The three-parameter incidence function kS^pI^q of the full HM model may not have sufficient flexibility to adequately fit the cyclic incidence pattern of the stochastic system. We emphasize here that if the cycles are not generated intrinsically, but are driven by an external variable such as a periodic environmental forcing, the outcome is well predicted when an appropriate forcing term is included in Eq. (2) (results not shown).

As a final note, all of the above observations for both stable equilibria and cyclic epidemic patterns have been qualitatively validated for multiple sets of values of the disease parameters β, γ and δ.

5. Discussion

Stochastic SIRS dynamics implemented on a network with varying degrees of local clustering can generate a rich spectrum of behaviors, including stable and noisy endemic equilibria as well as decaying and persistent cycles. Persistent cycles arise in our system even though the homogeneous mean-field dynamics do not have oscillatory solutions, thereby revealing an interesting interplay of network structure and disease dynamics (also see Rand, 1999). Our results demonstrate that a three-variable epidemic model with a nonlinear incidence function kS^pI^q, consisting of three "heterogeneity" parameters [k, p, q], is capable of predicting the disease transmission patterns, including the transient and stable equilibrium prevalence, in a clustered network. The relatively simpler (and more standard) form $S^{p_r}I^{q_r}$ with two

parameters $[p_r, q_r]$ falls short in this regard. This restrictive model, however, is an adequate predictor of the dynamics in a random network, for which the bilinear mean-field approximation cannot explain the transient pattern. Interestingly, even the function kS^pI^q cannot capture the complex dynamics of persistent cycles in a small-world network that has simultaneously high local clustering and long-distance connectivity. It is worth noting, however, that such persistent cycles appear within a small region of the parameter space for ϕ, and therefore the HM model appears to provide a reasonable approximation for most cases of clustered as well as randomized networks.

An implication of these findings is that an approximate relationship is established early on in the transients, lasting all the way to equilibrium, between the covariance structure of the [SI] pairs and the global (mean) quantities S and I. This relationship is given by a double power law of the number of susceptible and infective individuals. It allows the closure of the equations for mean quantities, making it possible to approximate the stochastic dynamics with a simple model (HM) that mimics the basic formulation of the mean-field equations but with modified functional forms. It reveals an interesting scaling pattern from individual to population dynamics, governed by the underlying contact structure of the network. In lattice models for antagonistic interactions, which bear a strong similarity to our stochastic disease system, a number of power-law scalings have been described for the geometry of the clusters (Pascual et al., 2002). It is an open question whether the exponents for the dynamic scaling (i.e., parameters p and q here) can be derived from such geometrical properties. It also needs to be determined under what conditions power-law relationships will hold between local structure and global quantities.

The failure of the HM model to generate persistent cycles may result from an inappropriate choice of the incidence function kS^pI^q. It remains to be seen if there exists a different functional form that better fits the incidence rate of the stochastic system and is capable of predicting the variability in the data. It is also not known whether a moment closure method including the explicit dynamics of the covariance terms themselves (Pacala and Levin, 1997; Keeling, 1999) can provide a good approximation to the mean infection level in a network with high degree of local clustering. Of course, heterogeneities in space or in contact structure are not the only factors contributing to the nonlinearity in the transmission function S^pI^q; a number of other biological mechanisms of transmission can lead to such functional forms. By rewriting βkS^pI^q as $[\beta kS^{p-1}I^{q-1}]SI \equiv \hat{\beta}SI$, where $\hat{\beta}(S, I)$ now represents a density-dependent transmission efficiency in the bilinear (homogeneous) incidence framework, one can relate $\hat{\beta}$ to a variety of density-dependent processes such as those involving vector-borne transmission, or threshold virus loads etc (Liu et al., 1986). Interestingly, it has been suggested that in such cases cyclic dynamics are likely to be stabilized, rather than amplified, by nonlinear transmission (Hochberg, 1991). It appears then that network structure can contribute to the cyclic behavior of diseases with relatively simple transmission dynamics.

It is interesting to consider the persistent cycles we have discussed here in light of other studies on fluctuations in networks. On one side, cycles have been described for random networks with $\phi = 1$ because the corresponding well-mixed dynamics also have oscillatory solutions (Lago-Fernández et al., 2000; Kuperman and Abramson, 2001). At the opposite extreme, Johansen (1996) reported persistent fluctuations in a stochastic SIRS model on a regular grid ($\phi = 0$), strictly generated by the local clustering of the grid since the mean-field equations do not permit cycles. Recent work by Verdasca et al. (2005) extends Johansen's observation by showing that fluctuations do occur in clustered networks from a regular grid to the small-world configuration. They describe a percolation type transition across the small-world region, implying that the fluctuations fall off sharply within this narro terval. This observation is in significant contrast to our results, where the amplitudes of the cycles are maximized by the small-world configuration, and therefore require both local clustering and some degree of randomization. One difference between the two models is that Verdasca et al. (2005) use a discrete time step for the recovery of infected individuals, while in our event-driven model, time is continuous and the recovery time is exponentially distributed. A more systematic study of parameter space for these models is warranted.

We should also mention that there are other ways to generate a clustered network than a small-world algorithm. For example, Keeling (2005) described a method that starts with a number of randomly placed focal points in a two-dimensional square, and draws a proportion of them towards their nearest focal point to generate local clusters. Network building can also be attempted from the available data on selective social mixing (Morris, 1995). The advantage of our small-world algorithm is that besides being simple to implement, it is also one of the best studied networks (Watts, 2003). This algorithm generates a continuum of configurations from a regular grid to a random network, and many real systems have an underlying regular spatial structure, as in the case of hantavirus of wild rats within the city blocks of Baltimore (Childs et al., 1988). Moreover, emergent diseases like the recent outbreak of severe acute respiratory syndrome (SARS) have been studied by modeling human contact patterns using small-world networks (Masuda et al., 2004; Verdasca et al., 2005).

The network considered here remains static in time. While this assumption is reasonable when disease spreads rapidly relative to changes of the network itself, there are many instances where the contact structure would vary over comparable time scales. Examples include group dynamics in wildlife resulting from schooling or spatial aggregation, as well as territorial behavior. Dynamic network structure involves processes such as migration among groups that establishes new connections and destroys existing ones, but also demographic processes such as birth and death as well as disease induced mortality. Another topic of current interest is the effect of predation on disease growth, which splices together predator–prey and host–pathogen dynamics in which the prey is an epidemic carrier (Ostfeld and Holt, 2004). Simple dynamics assuming the homogeneous mixing of prey and predators makes interesting predictions about the harmful effect of predator control in aggravating disease prevalence with potential spill-over effects on humans (Packer et al., 2003; Ostfeld and Holt, 2004). It remains to be seen if these

conclusions hold under an explicit modeling framework that binds together the social dynamics of both prey and predator. More generally, future work should address whether modified mean-field models provide accurate simplifications for stochastic disease models on dynamic networks. So far the work presented here for static networks provides support for the empirical application of these simpler models to time series data.

Acknowledgements

We thank Juan Aparicio for valuable comments about the work, and Ben Bolker and an anonymous reviewer for useful suggestions on the manuscript. This research was supported by a Centennial Fellowship of the James S. McDonnell Foundation to M.P.

Appendix A

A note on types of random networks

It is important to distinguish among the different types of random networks that are used frequently in the literature. One is the random network with $\phi = 1$ that is generated using the small-world algorithm as described in Section 2 (Fig. 1C), which has a total $Nn_0/2$ distinct connections, where n_0 is the original neighborhood size (=8 here) in the regular grid and N is the size of the network. Each individual in this random network has a binomially distributed number of contacts around a mean n_0. There is also the homogeneous random network discussed in relation to the mean-field Eq. (4), which by definition has fixed n_0 random contacts per individual (Keeling, 1999). These two networks are, however, different from the random network of Erdős and Rényi (Albert and Barabási, 2002), generated by randomly creating connections with a probability p among all pairs of individuals in a population. The expected number of distinct connections in the population is then $pN(N-1)/2$, and each individual has a binomially distributed number of connections with mean $p(N-1)$. For moderate values of p and large population sizes, the Erdős–Rényi network is much more densely connected than the first two types. All three of them, however, have negligible clustering C and path length L, since the individuals do not retain any local connections (all connections are short-cuts).

Appendix B

Details of model implementation

An appropriate network is constructed with a given ϕ, and the stochastic SIRS dynamics are implemented on this network using the rules described in Section 2. For the initial conditions, we start with a random distribution of a small number of infective individuals, only 0.5% of the total population (=0.005N) unless otherwise stated, in a pool of susceptible individuals. All generated time series used for least-squared fitting of the transmission rate have a length of 20,000 time units. The structure of the network remains fixed during the entire stochastic run. Stochastic simulations were carried out with a series of network sizes ranging from $N = 10^4$–10^6. The results presented here are those for $N = 160{,}000$ and are representative of other sizes. The values for the epidemic rate parameters β, γ and δ are chosen so that the disease successfully establishes in the population (a finite fraction of the population remains infected at all times).

REFERENCES

Albert, R., Barabási, A.L., 2002. Statistical mechanics of complex networks. Rev. Mod. Phys. 74, 47–97.
Anderson, R.M., May, R.M., 1992. Infectious Diseases of Humans: Dynamics and Control. Oxford University Press, Oxford.
Bailey, N.T., 1975. The Mathematical Theory of Infectious Diseases. Griffin, London.
Bjørnstad, O.N., Finkenstädt, B.F., Grenfell, B.T., 2002. Dynamics of measles epidemics: estimating scaling of transmission rates using a time series SIR model. Ecol. Monogr. 72, 169–184.
Bolker, B.M., 1999. Analytic models for the patchy spread of plant disease. Bull. Math. Biol. 61, 849–874.
Bolker, B.M., Grenfell, B., 1995. Space, persistence and dynamics of measles epidemics. Philos. Trans. R. Soc. Lond. Ser. B 348, 309–320.
Brown, D.H., Bolker, B., 2004. The effects of disease dispersal and host clustering on the epidemic threshold in plants. Bull. Math. Biol. 66, 341–371.
Childs, J.E., Glass, G.E., Korch, G.W., LeDuc, J.W., 1988. The ecology and epizootiology of hantaviral infections in small mammal communities of Baltimore: a review and synthesis. Bull. Soc. Vector Ecol. 13, 113–122.
Cliff, A.D., Haggett, P., 1984. Island epidemics. Sci. Am. 250, 138–147.
Dorogotsev, S.N., Mendes, J.F., 2003. Evolution of Networks. Oxford University Press, Oxford.
Eames, K.T.D., Keeling, M.J., 2002. Modelling dynamic and network heterogeneities in the spread of sexually transmitted disease. PNAS 99, 13330–13335.
Finkenstädt, B.F., Bjørnstad, O.N., Grenfell, B.T., 2002. A stochastic model for extinction and recurrence of epidemics: estimation and inference for measles outbreaks. Biostatistics 3, 493–510.
Franc, A., 2004. Metapopulation dynamics as a contact process on a graph. Ecol. Complex. 1, 49–63.
Gang, H., Ditzinger, T., Ning, C.Z., Haken, H., 1993. Stochastic resonance without external periodic force. Phys. Rev. Lett. 71, 807–810.
Grenfell, B.T., Harwood, J., 1997. (Meta) population dynamics of infectious diseases. Trends Ecol. Evol. 12, 395–399.
Gubbins, S., Gilligan, C.A., 1997. A test of heterogeneous mixing as a mechanism for ecological persistence in a disturbed environment. Proc. R. Soc. Lond. B 264, 227–232.
Hethcote, H.W., van den Driessche, P., 1991. Some epidemiological models with nonlinear incidence. J. Math. Biol. 29, 271–287.
Hochberg, M.E., 1991. Non-linear transmission rates and the dynamics of infectious disease. J. Theor. Biol. 153, 301–321.
Johansen, A., 1996. A simple model of recurrent epidemics. J. Theor. Biol. 178, 45–51.
Keeling, M.J., Rand, D.A., Morris, A.J., 1997. Correlation models for childhood epidemics. Proc. R. Soc. Lond. B 264, 1149–1156.

Keeling, M.J., 1999. The effects of local spatial structure on epidemiological invasions. Proc. R. Soc. Lond. B 266, 859–867.
Keeling, M.J., 2005. The implications of network structure for epidemic dynamics. Theor. Popul. Biol. 67, 1–8.
Kermack, W.O., McKendrick, A.G., 1927. A contribution to the mathematical theory of epidemics. Proc. R. Soc. Lond. A 115, 700–721.
Koelle, K., Pascual, M., 2004. Disentangling extrinsic from intrinsic factors in disease dynamics: a nonlinear time series approach with an application to cholera. Am. Nat. 163, 901–913.
Koopman, J., 2004. Modeling infection transmission. Ann. Rev. Pub. Health 25, 303–326.
Kuperman, M., Abramson, G., 2001. Small world effect in an epidemiological model. Phys. Rev. Lett. 86, 2909–2912.
Lago-Fernández, L.F., Huerta, R., Corbacho, F., Siguenza, J.A., 2000. Fast response and temporal coherent oscillations in small-world networks. Phys. Rev. Lett. 84, 2758–2761.
Liu, W., Levin, S.A., Iwasa, Y., 1986. Influence of nonlinear incidence rates upon the behavior of SIRS epidemiological models. J. Math. Biol. 23, 187–204.
Liu, W., Hethcote, H.W., Levin, S.A., 1987. Dynamical behavior of epidemiological models with non-linear incidence rate. J. Math. Biol. 25, 359–380.
McCallum, H., Barlow, N., Hone, J., 2001. How should pathogen transmission be modelled? Trends Ecol. Evol. 16, 295–300.
Maule, M.M., Filipe, J.A.N., in preparation. Relating heterogeneous mixing models to spatial processes in disease epidemics.
Masuda, N., Konno, N., Aihara, K., 2004. Transmission of severe acute respiratory syndrome in dynamical small-world networks. Phys. Rev. E 69, 031917(1–6).
Morris, M., 1995. Data driven network models for the spread of disease. In: Mollison, D. (Ed.), Epidemic Models: Their Structure and Relation to Data. Cambridge University Press, Cambridge, pp. 302–322.
Murray, J.D., 1993. Mathematical Biology. Springer-Verlag, Berlin.
Newman, M.E.J., 2002. The spread of epidemic disease on networks. Phys. Rev. E 66, 016128(1–11).
Newman, M.E.J., Watts, D.J., 1999. Scaling and percolation in the small-world network model. Phys. Rev. E 60, 7332–7342.
Ostfeld, R.S., Holt, R.D., 2004. Are predators good for your health? Evaluating evidence for top-down regulation of zoonotic disease reservoirs. Front. Ecol. Environ. 2, 13–20.
Pacala, S.W., Levin, S.A., 1997. Biologically generated spatial pattern and the coexistence of competing species. In: Tilman, D., Kareiva, P. (Eds.), Spatial Ecology. Pinceton University Press, Princeton, NJ, pp. 204–232.
Packer, C., Holt, R.D., Dobson, A., Hudson, P., 2003. Keeping the herds healthy and alert: impacts of predation upon prey with specialist pathogens. Ecol. Lett. 6, 797–802.
Pascual, M., Rodó, X., Ellner, S.P., Colwell, R., Bouma, M.J., 2000. Cholera dynamics and EL Niño-Southern Oscillation. Science 289, 1766–1769.
Pascual, M., Roy, M., Franc, A., 2002. Simple temporal models for ecological systems with complex spatial patterns. Ecol. Lett. 5, 412–419.
Pastor-Satorras, R., Vespignani, A., 2001. Epidemic spreading in scale-free networks. Phys. Rev. Lett. 86, 3200–3203.
Rand, D.A., 1999. Correlation equations and pair approximations for spatial ecologies. In: McGlade, J. (Ed.), Advanced Ecological Theory: Principles and Applications. Blackwell Sc., London, pp. 100–142.
Rhodes, C.J., Anderson, R.M., 1996. Persistence and dynamics in lattice models of epidemic spread. J. Theor. Biol. 180, 125–133.
Sander, L.M., Warren, C.P., Sokolov, I.M., Simon, C., Koopman, J., 2002. Percolation on heterogeneous networks as a model for epidemics. Math. Biosci. 180, 293–305.
Severo, N.C., 1969. Generalizations of some stochastic epidemic models. Math. Biosci. 4, 395–402.
Shirley, M.D.F., Rushton, S.P., 2005. The impacts of network topology on disease spread. Ecol. Complex. 2, 287–299.
Smith, K.F., Dobson, A.P., McKenzie, F.E., Real, L.A., Smith, D.L., Wilson, M.L., 2005. Ecological theory to enhance infectious disease control and public health policy. Front. Ecol. Environ. 3, 29–37.
Van Baalen, M., 2002. Contact networks and the evolution of virulence. In: Dieckmann, U., Metz, J.A.J., Sabelis, M.W., Sigmund, K. (Eds.), Adaptive Dynamics of Infectious Diseases. Cambridge University Press, Cambridge, pp. 85–103.
Verdasca, J., Telo da Gama, M.M., Nunes, A., Bernardino, N.R., Pacheco, J.M., Gomes, M.C., 2005. Recurrent epidemics in small world networks. J. Theor. Biol. 233, 553–561.
Watts, D., 2003. Small Worlds. Princeton University Press, Princeton, NJ.
Watts, D.J., Strogatz, S., 1998. Collective dynamics of small-world networks. Nature 363, 202–204.